Brigham Young University
BYU ScholarsArchive

Theses and Dissertations

2011-05-12

Possible Molecular Mechanism to Account for Wavelength Dependence of Equilibration Rates of Patman and Laurdan in Phosphatidylcholine Bilayers

Hannabeth A. Franchino
Brigham Young University - Provo

Follow this and additional works at: https://scholarsarchive.byu.edu/etd

Part of the Cell and Developmental Biology Commons, and the Physiology Commons

BYU ScholarsArchive Citation

Franchino, Hannabeth A., "Possible Molecular Mechanism to Account for Wavelength Dependence of Equilibration Rates of Patman and Laurdan in Phosphatidylcholine Bilayers" (2011). *Theses and Dissertations*. 3014.
https://scholarsarchive.byu.edu/etd/3014

This Thesis is brought to you for free and open access by BYU ScholarsArchive. It has been accepted for inclusion in Theses and Dissertations by an authorized administrator of BYU ScholarsArchive. For more information, please contact scholarsarchive@byu.edu, ellen_amatangelo@byu.edu.

Possible Molecular Mechanism to Account for Wavelength Dependence of Equilibration Rates of Patman and Laurdan in Phosphatidylcholine Bilayers

Hannabeth Franchino

A thesis submitted to the faculty of
Brigham Young University
in partial fulfillment of the requirements for the degree of

Master of Science

John D. Bell, Chair
Dixon J. Woodbury
David M. Belnap

Department of Physiology and Developmental Biology

Brigham Young University

June 2011

Copyright © 2011 Hannabeth Franchino

All Rights Reserved

ABSTRACT

Possible Molecular Mechanism to Account for Wavelength Dependence of Equilibration Rates of Patman and Laurdan in Phosphatidylcholine Bilayers

Hannabeth Franchino
Department of Physiology and Developmental Biology, BYU
Master of Science

Patman is a fluorescent membrane probe related to Laurdan. The structural distinctions between the two probes are the lengths of the aliphatic tails (eleven carbons in Laurdan and fifteen in Patman) and the presence of a trimethylammonium group on Patman that produces a positively-charged head. Preliminary studies exploring Patman as a probe to detect membrane properties during apoptosis revealed that the fluorescence intensity of two edges of the emission spectrum (435 and 500 nm) stabilizes at different rates as the probe binds to the cell membrane. To test whether these differences represent dissimilarities in probe binding to ordered and disordered domains, experiments were conducted to monitor Patman equilibration with bilayers composed of various mixtures of saturated and unsaturated phosphatidylcholines at temperatures above, at, and below the main thermotropic phase transition. In general, Patman equilibrated more rapidly with bilayers in the liquid-disordered phase than in the solid-ordered phase. With solid phase membranes, the fluorescence stabilized faster at 500 nm than at 435 nm. Similar, yet more subtle, results occurred in the lipid disordered phase. In contrast, the situation was reversed at the phase transition temperature; equilibration was faster at 435 nm than at 500 nm. To determine whether these results reflected specific properties of Patman, the experiments were repeated with Laurdan, and several distinctions were observed. First, equilibration with solid phase lipids was faster than for Patman and not different from equilibration with the fluid phase. Second, differences in rates between the two wavelengths were less than with Patman for solid phase membranes but greater than with Patman for melted bilayers. Third, at the phase transition temperature, the difference in equilibration rates was the opposite of the result obtained with Patman. Computer simulations were used to assist with interpretation of these results. The data suggest that both probes bind superficially to the membrane before incorporating among the lipid molecules. Once within the membrane, Patman localizes to at least two distinct depths within the bilayer. Probe molecules in the shallow, more hydrated position favor 500 nm emission and those occupying a deeper, dehydrated position emit primarily at 435 nm. Laurdan's equilibration additionally represents movement of the probe between leaflets and multiple bilayers.

Keywords: Patman, Laurdan, equilibration, wavelength, membrane, bilayer, dynamics, solid phase, liquid phase, phase transition

ACKNOWLEDGMENTS

Thank you to the Laboratory for Fluorescence Dynamics (LFD) at the University of Irvine, CA for generously allowing us use of their facilities. Also, thank you to Dr. John Bell, my committee chair, for his diligent and patient guidance and teaching throughout this project and during my four years as a part of his lab.

TABLE OF CONTENTS

LIST OF FIGURES v
INTRODUCTION 1
Chemistry and physics of the probes 1
Use of these probes in living cells 4
Justification for this project 5
MATERIALS & METHODS 6
Formation of vesicles 6
Time courses 8
Analysis 9
Simulations 9
Cultured Cells 10
RESULTS 11
Differential equilibration in cells 11
Spectra of probes in vesicles 12
Kinetics of time courses 13
Simulations 16
DISCUSSION 17
Overview 17
Model 18
Saturated vs. Unsaturated Lipids 21
Summary 22
WORKS CITED 37

LIST OF FIGURES

Figure 1.....23

Figure 2.....24

Figure 3.....25

Figure 4.....26

Figure 5.....27

Figure 6.....28

Figure 7.....29

Figure 8.....30

Figure 9.....31

Figure 10.....32

Figure 11.....33

Figure 12.....34

Figure 13.....35

Figure 14.....36

Possible Molecular Mechanism to Account for Wavelength Dependence of Equilibration Rates of Patman and Laurdan in Phosphatidylcholine Bilayers

INTRODUCTION

Chemistry and physics of the probes

Fluorescence spectroscopy is a valuable biological technique that allows one to use small fluorescent molecules to investigate many properties of living cells including membrane structure and organization. One family of these fluorescent molecules includes the naphthalene probes Prodan, Laurdan, and Patman. All three of these dyes share an identical chromophore but differ enough structurally that each probe locates at different positions in the headgroup regions of membranes [1]. (Figure 1 displays the structural differences of these molecules, as well as their relative location in the bilayer composed of 1,2-dioleoyl-s*n*-glycero-3-phosphocholine (DOPC) [1].) Prodan is the smallest of these probes, while Laurdan and Patman are modified to better anchor them to a specific location in the membrane [2]. Laurdan has an 11-carbon tail attached to the carbonyl group of the fluorophore; stabilization of the tail in the hydrophobic region of the membrane sets the fluorophore location level with the glycerol backbone [2]. Patman, which also has a hydrophobic tail (15 carbons), has a trimethylammonium group on the opposite end of the aromatic rings of the fluorophore, ensuring that the alkylamino end of the fluorophore is oriented toward the lipid-water interface in the membrane and remains in the hydrophilic region of the membrane [2-4]. These differences in membrane

localization among the probes appear to be consistent in both mixed and pure lipid bilayers [1].

Of the three probes, Patman's movement is most restricted, and it is proposed to reside in the most homogenous microenvironment in the membrane [1-3, 5]. It sits at the level of the sn-1-ester group of the phospholipid regardless of the length of the lipid tail, keeping it the same distance from the lipid water interface even when the membrane composition varies [3]. Consequently, it is typically used in solvent relaxation studies of neutral lipids [3]. Such studies have shown that Patman elucidates both the number and motion of bound water molecules residing in the carbonyl region of the bilayer (between the fluorophore and the 15 carbon tail) [6]. The solvent relaxation that occurs causes a red shift in Patman's emission spectrum [5] and is known to take place on the timescale of nanoseconds [7]. The spectra of Patman exhibit few differences between both small unilamellar vesicles (SUV) and multilamellar vesicles (MLV), and fluorescent studies have shown no evidence that the probe aggregates in aqueous solution, which is an expected result due to its charged trimethylammonium group [5, 8]. It is not yet known whether Patman preferentially partitions in the different lipid phases in the membrane [9].

Both Patman and Laurdan exhibit many similarities, as they have very low solubility in water (unlike Prodan), partition strongly into lipid bilayers, and are able to detect temperature-induced membrane phase transitions. The emission spectra of Laurdan at various temperatures has been well studied and is known to be centered around 430 nm with the membrane in the lipid gel phase and display a wide band near 490 nm in the fluid, liquid-crystalline phase [10]. Our preliminary research, as well as other published results, indicates a similar pattern in the spectra of Patman; though, contrary to those of

Laurdan, these spectra are not as well studied or characterized. These characteristics make both probes useful in reporting the structure of membranes [1, 9, 11].

A number of studies have been carried out to determine the location of these probes among the head groups of phospholipids in the membrane [2, 5, 8]. Both Laurdan and Patman have been reported to lie at the glycerol backbone but do not both reside at identical positions. In a DOPC membrane, the fluorophore of Laurdan resides 11.4 Å from the bilayer center, while that of Patman sits deeper, 10.4 Å from the center [2]. Though the separation of membrane position of a single angstrom may not seem a significant difference between these probes, the degree of water penetration seems to vary greatly between these locations [3, 10]. Thus, the behavior of the probes may be distinct due to differences in hydration at the location of the fluorophore, as the amount of water affects the emission wavelength due to solvent relaxation.

As mentioned previously, the phenomenon of solvent relaxation also affects the fluorescence of these probes in the membrane. Solvent relaxation occurs when the dipole of the fluorophore changes both magnitude and direction as the excited electron moves from its ground state to a higher energy level. (This shift in the distribution of charge for Patman and Laurdan is approximately 20 D (C/m^2), which is similar to a 4 Å separation of unit electrical charge [12, 13].) Such excitation creates a new temporary dipole in the fluorophore, which causes the mobile dipoles (water or other solvent) around the molecule to reorient and align with the new charge vector. Such organization of water molecules causes a decrease in entropy of the system, resulting in a reduction of the energy of the excited state of the probe, thereby increasing the wavelength of the emission of the probe [5]. (The approximate red shift of the peak is from 420-430 nm to

480-500 nm.) Due to the occurrence of solvent relaxation, these probes are sensitive to the amount of water in the membrane. Thus, as the lipids undergo phase changes, which result in an increase of the ability of water to penetrate the membrane, both Patman and Laurdan are able to detect and report these membrane changes.

Preliminary studies in our laboratory exploring Patman as a probe to detect membrane properties during apoptosis revealed that the intensity of emitted light at the two edges of the emission spectrum (435 and 500 nm) stabilized at different rates as the probe binds to the cell membrane. Laurdan has also shown varying equilibration rates at the two emission wavelengths. These differences between wavelengths may indicate dissimilarities in probe binding to ordered and disordered domains, changes due to probe equilibration between membrane leaflets, or some other difference in membrane properties and the probe's interaction with the membrane.

Use of these probes in living cells

Laurdan is a commonly used probe, found in fluorescence energy transfer, FTIR, red edge excitation shift, and of course, fluorescence spectroscopy experiments [2, 14-16]. It is commonly used to detect phase transitions, membrane hydration, and lipid packing. Patman is used less extensively but has been found to be useful in fluorescence spectroscopy and ^{1}H-NMR experiments to determine polarity and rigidity changes in membranes [3, 5, 8]. None of these studies with either probe have studied the equilibration of these fluorophores at more than one wavelength.

Justification for this project

The purpose of this research project is to understand the properties of the probes and apply that knowledge to experiments with living cells. Both Laurdan and Patman are often used to study cellular membranes, specifically, membrane order. However, they are typically added to the system and allowed several minutes to equilibrate before their fluorescence is measured. This protocol misses all the possible data that could be gathered from the membranes while the fluorophore equilibrates. Thus, by looking at equilibration of the probes in the membrane, more information can be gained than by assaying only the endpoint fluorescence. As previously alluded to, preliminary studies investigating apoptosis and necrosis using fluorescent probes Patman and Laurdan have detected these unequal equilibration rates of the molecules' wavelengths. This ability to detect changes in the membrane structure that occurs during cell death is evidence that some unknown information about the changing membrane states is being gathered by these probes. However, without a proper understanding of the nature of the fluorescent molecules and their accompanying wavelength equilibration dynamics, interpretation of these results is limited or impossible. Additionally, as the data seems to indicate variation in equilibration when the membrane is changing or existing as domains, an increased understanding of Patman and Laurdan will be useful for a variety of facets of biophysics involving membrane domains, including lipid raft research, superlattice structures, or vesicle trafficking, in addition to the application to cell death (specifically, apoptosis or necrosis). Our study has aided in the application of this acquired understanding by carrying out a number of 2-photon microscopy experiments using murine lymphoma cells and the two probes in both healthy and dying cells. The results indicate that the differences in equilibration dynamics, both between the two wavelengths and between the

two probes, do exist when applied to living cells. These results can be imaged and the changes viewed over time as a short movie. It is clear that the behavior studied in artificial membranes with respect to both probes does exist in living cells and is important in a number of areas of biophysics research.

In addition to the biological context of this research, an understanding of these probe's equilibration dynamics represents a valuable addition to the field of biophysics by providing a more detailed understanding of these commonly used fluorescent molecules. It explores a gap in understanding of these fluorescent tools, which, an advanced understanding of, will likely aid and enhance research into membrane changes during cell death. Additionally, the design of these experiments and application of these probes in this manner represent a novel addition to the field of fluorescent spectroscopy, as very little has been done investigating the changes in kinetics or equilibration dynamics of probes over time. Research providing a more in-depth understanding of properties and use of another fluorescent probe, merocyanine 540, was recently published, indicating an interest and application of this type of research in the field of biophyisics [17].

MATERIALS & METHODS

Formation of vesicles

MLVs – Vesicles were made using various phosphatidylcholines (both saturated and unsaturated) to create both pure (100% 1,2-dipalmitoyl-*sn*-glycero-3-phosphocholine (DPPC), 1,2-dimyristoyl-*sn*-glycero-3-phosphocholine (DMPC), 1,2-distearoyl-*sn*-glycero-3-phosphocholine (DSPC), 1,2-dioleoyl-*sn*-glycero-3-phosphocholine (DOPC),

1-palmitoyl-2-oleoyl-*sn*-glycero-3-phosphocholine (POPC)) (Avanti Polar Lipids, Birmingham, AL) and mixed (50% DMPC-50% DSPC, 25% DMPC-75% DSPC, 75% DMPC-25% DSPC, 50% POPC-50% DPPC, 25% POPC-75% DPPC, 75% POPC-25% DPPC, 50% DOPC-50% DPPC, 25% DOPC-75% DPPC, 75% DOPC-25% DPPC) lipid systems. All lipids were dissolved in chloroform (DPPC (20 mg/ml; MW = 734 g/mole), DMPC (10 mg/ml; MW = 677.94 g/mole), DSPC (10 mg/ml; MW = 790.15 g/mole), DOPC (25 mg/ml; 786.15 g/mole), POPC (10 mg/ml; MW = 760.10 g/mole)) and stored at low temperatures in properly sealed, non-reactive containers. Samples were prepared in the correct concentration so each experimental sample will contain 1 µmole total lipid (1 component systems: 3.6 µl DPPC; 7.3 µl DMPC; 7.9 µl DSPC; 7.6 µl POPC; 3.1 µl DOPC; 2 component systems: 3.4 µl DMPC with 4.0 µl DSPC; 1.7 µl DMPC with 5.10 µl DSPC; 5.1 µl DMPC with 2.0 µl DSPC; 3.8 µl POPC with 1.8 µl DPPC; 1.9 µl POPC with 2.8 µl DPPC; 5.7 µl POPC with 0.9 µl DPPC; 1.6 µl DOPC with 1.8 µl DPPC; 0.80 µl DOPC with 2.8 µl DPPC; 2.4 µl DOPC with 0.9 µl DPPC). Samples were dried under N_2 gas and resuspended in 2 ml of citrate buffer (20 mM sodium citrate/citric acid, 150 mM KCl, pH 7). Suspensions were incubated six times in a shaking water bath at ≥ 50 °C or ≥ 60 °C (for all samples containing DSPC) at 10-min intervals and dispersed by vortex mixing between each incubation (for a total incubation time of 1 h). The average size of the MLVs, as measured by light scatter experiments (Brookhaven, 90Plus Particle Size Analyzer), was 1070 nm (half width = 520 nm; polydispersity = 0.260). Vesicles were stored in a covered container at room temperature and suspended by vortex mixing immediately before use to ensure uniform distribution within the 2 ml sample volume.

LUVs – Unilamellar vesicles were created for both the pure and mixed membrane systems of the saturated lipids. They were created more concentrated than the MLVs in a volume of 3 ml such that a 100 µL aliquot of the samples will contain 1 µmole total lipid (100% DPPC (110.1 µl); 100% DMPC (203.4 µl); 100% DSPC (237.0 µl); 50% DMPC-50% DSPC (110.7 µl, 118.5 µl, respectively); 75% DMPC-25% DSPC (152.6 µl, 59.3 µl, respectively); 25% DMPC-75% DSPC (50.9 µl, 177.8 µl, respectively)). The lipids were again dried, lyophilized overnight, resuspended in buffer, and incubated in a high temperature water bath (and periodically dispersed by vortex mixing) for an hour. Following incubation, samples were extruded 6 – 10 times through a 100 nm polycarbonate filter in a pressured extruder heated with a circulating waterbath above the lipid's phase transition (≥ 50 °C for DMPC and DPPC vesicles; ≥ 60 °C for any DSPC vesicles). The average size of LUVs, as measured by light scatter experiments, was 128 nm (half width = 36 nm; polydispersity = 0.080). Vesicles were stored and suspended in the same manner as MLVs.

Time courses

Experiments were carried out on a photon-counting spectrofluorometer (Horiba Jobin-Yvon). Samples were incubated for 10 min at a given temperature between 18 and 60 °C to ensure temperature equilibration of each sample prior to collecting a measurement. Following temperature equilibration, a 1000 s time course experiment was carried out (excitation – 350 nm; emission – 435 and 500 nm) to examine the equilibration dynamics of Patman or Laurdan. During each time course, background fluorescence was collected in the first 100 s for the samples lacking either probe. At 100

s, 0.86 µl Patman or Laurdan (580 mM) were added, and the time course continued for another 900 s, allowing collection of fluorescent emission values of the probe as it equilibrates with the membrane. Spectra of the vesicles were also collected across the temperature range.

Analysis

Time course data were analyzed and fit by non-linear regression ($A(1 - e^{-bt}) + C(1 – e^{-dt}) + Et + F$) using Prism analysis software. The derivatives of the fits ($Abe^{-bt} + Cde^{-dt} + E$) for each temperature at both 435 and 500 nm were calculated in order to compare the differences in the equilibration rates. The rates were then normalized to end point fluorescence, and the difference between these normalized rates (R) for the two wavelengths was determined (difference = $R_{435\ nm} – R_{500\ nm}$). This analysis method allowed changes in probe's fluorescence over time to be assessed without the relative quantity of fluorescence at each wavelength clouding the differences or similarities in the molecule's rate of equilibration.

Simulations

Numerical integration simulations were carried out in order to aid understanding of time course results. The model that accurately described our experimental results involved two membrane compartments, denoted as Membrane A and Membrane B (Figure 2). However, it seems there are two positions of the probe even when integrated into a homogenous membrane system, following an initial or superficial binding. A more stable, non-superficial binding of the molecule seems to occur at two locations along the

acyl chain of the lipids, creating two probe populations. The differences in the binding or populations of the probe are designated as A and B. In this model, we assume the probe begins in an aqueous solution, and then initially or superficially binds to the membrane. Following that initial binding, the probe is able to equilibrate to deeper regions of the membrane (A or B) and able to move between membrane compartments (from A to B or B to A). Thus, there exist 4 reversible equilibration pathways for the molecules to follow. As each reversible pathway consists of a forward and reverse of movement, there are 8 rate constants in the simulation describing the general motion of the fluorophore in each direction (Figure 2). The relative fluorescence of each wavelength in each region (membrane A or B, aqueous, initial) was set with the highest total fluorescence occurring in the membrane A or B compartments and the lowest in the aqueous, as both probes are known to minimally fluoresce in aqueous solutions [5, 10].

Cultured Cells

Experiments with S49 murine lymphoma cells were carried out, allowing us to image the probes' equilibration by using 2-photon microscopy. These experiments were done at the Laboratory for Fluorescence Dynamics (LFD) at the University of Irvine, CA. The cells were cultured in a suspension of Dulbecco's modified Eagle medium (DMEM), which contained 10% inactivated horse serum, at 37 C and 10% CO2 [18, 19]. Cells were collected using gentle centrifugation and were then washed and suspended in a salt medium (MBSS: NaCl = 134 mM, KCl = 6.2 mM, CaCl2 = 1.6 mM, MgCl2 = 1.2 mM, Hepes = 18.0 mM, and glucose 13.6 mM, pH 7.4, 37 °C) [18, 19]. Two ml of cells were added to a microscopy dish and incubated at 37 C for 5 min. If a culture was treated with

the calcium ionophore, ionomycin, 5 µl (120 µM) were added and an additional 10 min passed before beginning the 2-photon scan. The excitation for the microscope was set to 780 nm and the probe (0.86 µl of either Patman (580 µM) or Laurdan (580 µM)) was added immediately before the 2-photon scan began. Between 50-100 scans were collected each run, creating an image of each probe's equilibration over approximately 5-10 min.

RESULTS

Differential equilibration in cells

Examination of the fluorescence of Patman with living cells revealed differences in the equilibration of the probe with the membrane for the two edges of the emission spectrum, measured at 435 and 500 nm. Time course experiments with normal cells showed a clear difference in the equilibration kinetics of the data acquired at 435 nm compared to 500 nm (Figure 3, upper panel). These differences were best visualized by computing the derivative of each time course, normalizing to its total intensity increase, and calculating the difference between the two normalized derivatives (Figure 3, upper panel, black curve). The pattern of the kinetics, as revealed by the black curve, varied according to the treatment or state of the cells. Thus, when the cells were treated with an apoptotic agent, thapsigargin, the time profile of the derivative difference was markedly altered compared to control (see Figure 3, lower panel). One possible explanation for the slow and differential kinetics at the two wavelengths is that Patman penetrates at different rates into various subcellular compartments with molecular environments that promote greater fluorescence intensity at one wavelength versus the other. In order to address this question for living cells, two-photon imaging experiments were carried out at the two

wavelengths. As shown in Figures 4, Patman stained only the cell membrane at both wavelengths. This result validates predictions from previous studies that Patman, due to its positive charge, should only equilibrate with and stain the plasma membrane (likely, only the outer leaflet) of the cell [8]. Conversely, Laurdan, which lacks the positive charge, diffuses through the plasma membrane to stain both leaflets and the membranes of cellular organelles [20].

We wanted to investigate both the differences between the behavior of the individual wavelengths and between the two probes. However, due to the complexity of cellular membranes, it seemed unlikely that clear, interpretable results would be possible using living cells. Thus, we created artificial bilayers of various compositions in order to better understand the behavior and properties of the probes.

Spectra of probes in vesicles

In order to verify that Patman is sensitive to the phase transitions of the lipids, spectra were collected from 400−600 nm across a range of temperatures below, at, and above the phase transition. The DPPC spectra for Patman showed an iso-emissive point between the low (18, 25 °C) and high temperatures (45, 50 °C), suggesting that the spectra at each temperature represent relative contributions of two primary populations (Figure 5). At and around the phase transition temperature (T_m = 41.5 °C), the spectra are greater in width and blur the iso-emissive point (41−43 °C) (Figure 5). In the case of this lipid, it would appear that the population centered at about 430 nm represents solid-phase lipid, and the one centered at approximately 475 nm represents liquid-phase lipid. Thus, Patman is able to distinguish between the solid and liquid-crystalline phases of the DPPC

membrane. This outcome is analogous to results obtained with Laurdan as previously published [10].

Additionally, when the choice of lipid (and consequently, the temperature of the phase transition) is altered, Patman remains capable of detecting phase transitions. A pattern similar to that seen with DPPC occurred with both DMPC (T_m = 26−29 °C) and DSPC (T_m = 54 °C) (Figure 6). When lipid mixtures at incremental ratios of DMPC and DSPC were created, predictable shifts in the spectra occurred. Each ratio showed a group of shorter wavelength peaks at low temperatures, matching those seen in pure DMPC vesicles, and a group of longer wavelength peaks at high temperatures, like those in pure DSPC vesicles. At the intermediate temperatures (40−50 °C) above the phase transition of DMPC but below that of DSPC, spectra were shifted slightly, sat between the low and high temperature peaks, and showed more of a shoulder around 500 nm (Figure 7).

The spectra of unsaturated lipids mixed with DPPC were quite similar to those of pure DPPC. Due to the low phase transition temperature of DOPC (Tm = -20 °C) and POPC (Tm = -2 °C), they existed as fluid-phase domains at all the assayed temperatures. Thus, any changes detected by Patman were due to the changing state of the DPPC lipids. The most obvious difference between these spectra and those of only DPPC is that the peaks at the low temperatures seem to be broader than the pure systems', likely reflecting two coexisting probe populations, one solid and one liquid (Figure 8).

Kinetics of time courses

Time course experiments showed a clear difference in the rate of equilibration of Patman's intensity at each wavelength (435 and 500 nm) in vesicles composed of both

pure and mixed lipids. Figure 9 displays an example of this difference in a pure DPPC system at a low temperature (18 °C) with the intensity at 500 nm approaching equilibration sooner than that at 435 nm. At temperatures above the lipid phase transitions, this pattern of equilibration was different, as can be seen with pure DPPC vesicles at 48 °C where the two intensity curves more closely mirror one another (Figure 9). These equilibration curves for each time course were fit using non-linear regression, and the derivatives of the resulting curves were calculated. The difference between these derivative values for both wavelengths allowed comparison of changes in the rates of equilibration at each wavelength over time. The meaningful differences occurred early in the time course, and we therefore focused our attention on the first 400 s. These time course experiments and derivative analyses were carried out for pure and mixed-lipid vesicles, using saturated and unsaturated lipids (Figure 10). Additionally, the differences were studied using both MLV and LUV vesicles. No distinction could be made in the equilibration patterns between these two vesicle types (Two-way ANOVA, effect of vesicle type: solid phase: $p = 0.27$, phase transition: $p = 0.70$, liquid phase: $p = 0.48$; the other dimension was lipid type (see below); interaction was also insignificant in each case). Consequently, data for MLV and LUV were pooled for the remaining analyses.

The equilibration patterns of both Patman and Laurdan were compared by studying the differences in rate between the wavelengths in three states of the lipid membranes: solid, liquid, and at the phase transition. Figure 11 compares the equilibration of the two fluorophores in solid-ordered membranes. For both probes, the intensity at 435 nm equilibrated more slowly than at 500 nm where the rate of change often became zero by 400 s. Consequently, the difference in the rate of change (435 nm –

500 nm) was positive for both Patman and Laurdan. By 400 s, however, the rate difference for Laurdan was much closer to zero, meaning much closer to equilibration at both wavelengths. In contrast, the difference at 400 s for Patman was still similar to that at 200 s, indicating a slower equilibration for the charged probe.

When the behavior of the probes was studied in liquid-disordered membranes, several key differences were evident (Figure 12). First, when Patman was in a liquid membrane, whether saturated or unsaturated, the difference between 435 and 500 nm was smaller than in the solid phase. This reduced gap in equilibration rate appeared to reflect faster equilibration at 435 nm compared to that observed for solid lipids at the wavelength. Hence, the time profiles at the two wavelengths were parallel as suggested by the data in Figure 9. In contrast, the time profiles were not parallel for Laurdan as shown by the larger gap in equilibration rate and the fact that the gap was smaller at 400 s compared to 200 s in Figure 12. This result suggested that the slower approach to equilibrium at 435 nm obvious for both probes in the solid phase persisted into the liquid phase for Laurdan. Interestingly, the equilibration pattern for the two probes appeared to distinguish between vesicles that contained only saturated lipids in the liquid phase compared to those that contained at least 25% unsaturated lipids. When unsaturated lipids were used, the differences between rates at 435 and 500 nm were universally greater (Figure 12).

When allowed to equilibrate in saturated lipids at the phase transition temperatures, the two fluorophores differed even more (Figure 13). Only at the phase transition was the difference in rate for either probe consistently a negative value. As shown in Figure 13, these negative values were observed with Patman, but not Laurdan.

These results suggest that Patman's 435 nm emission intensity curve was approaching stability and therefore reaching a derivative of zero faster than the 500 nm emission intensity curve. Additionally, the magnitude of the negative difference for Patman depended on the length of the acyl chain of the lipid system in which the probe was equilibrating ($p = 0.0026$ at t = 100 s; $p = 0.028$ at t = 150 s, linear regression of rate difference *vs.* chain length, n = 24). DMPC (14:0) was the closest to zero at 150 s, while DSPC (18:0) was significantly more negative. For Laurdan, however, the difference in rate between the two wavelengths remained positive, as was true for the other two lipid phases. Thus, at the phase transition, the 435 nm intensity curve continued to equilibrate more slowly than the 500 nm intensity curve. Additionally, unlike Patman, there was no significant difference in the values among the three saturated lipids; instead, all of the values were approximately the same.

Simulations

The model developed and shown in Figure 2 was capable of replicating the salient features of the results. Figure 14 is an example of a simulated time course whose emission curve shapes closely match those shown in Figure 9. The parameter values for the equilibration constants are listed in the figure legend. Simpler models were attempted to describe the data but were insufficient to reproduce the basic results of a probe population emitting at 500 nm equilibrating faster than a population emitting at 435 nm. These simpler models included allowing the probe to move from the aqueous environment to two separate membrane positions or to move from the aqueous environment to a single membrane position before migrating to a second membrane

position. The features of the simulation that were necessary to reproduce the results were that the probe first absorbed to the membrane with initial binding before equilibrating into at least two different membrane states.

DISCUSSION

Overview

Our initial hypothesis based on preliminary data from cells (Figure 3) was that the differential rates of Patman equilibration at long and short emission wavelengths was due to compartmentalization of the probe into various membrane domains. It seemed reasonable that the molecular environment of one type of domain could cause the fluorophore to preferentially emit at 435 nm, while the other would produce greater emission at 500 nm. However, these experiments with vesicles demonstrate that varying equilibration patterns between the wavelengths are not due to the complexity of the membrane in which the molecule fluoresces. This non-matching equilibration pattern of the intensities at these two wavelengths occurred repeatedly and across a range of temperatures for both single and multi-component membranes. Additionally, the difference between the rates of equilibration at each wavelength was comparable for membrane systems that were either uni- or multi-lamellar. The mathematical model shown in Figure 2 was the simplest scenario we could create that would accurately simulate the experimental results. Simply having the probe move from the aqueous compartment to the membrane was insufficient, as was allowing the probe to move into discrete membrane compartments without an initial membrane adsorption. Taken together, it seems that it is not the membrane compartments themselves that cause this

equilibration pattern, but rather multiple populations of the fluorescent molecules that exist in even the simplest membrane systems.

Patman is sensitive to the solvent relaxation effect. Accordingly, its emission spectrum shifts toward longer wavelength depending on the amount of water or other polar molecules in its immediate environment [3]. By using the parallax quenching method, the average location of Patman relative to the center of a DOPC bilayer was assayed simultaneously with the wavelength of its emission peak [2, 3]. When the probe was deeper in the bilayer, meaning closer to the center, it emitted at 425-435 nm. Thus, when residing far from the surface of the lipids, its environment is fairly dehydrated. Conversely, when it sat closer to the lipid heads, its emission curve peaked between 490-510 nm. These data can be used to offer an interpretation of our results.

Model

Using both our mathematical model and our experimental data as a guide, it seems reasonable that this differential equilibration that occurs between emission wavelengths of the probe could be due to the depth of fluorophore populations in the bilayer. If so, the likely sequence of events would be as follows: Upon being introduced into the aqueous solution at $t = 0$, Patman quickly moves to the surrounding bilayers, which provide a much more favorable environment for the molecule due to its long, non-polar chain. Based on the low intensity emission early in the time course, Patman probably first binds superficially when it initially interacts with the bilayer. This initial binding will keep the probe in a very hydrated state and result in the majority of its fluorescence being emitted at a longer wavelength, the solvent relaxed state. Furthermore,

it appears that this state is quite stable since migration away from it requires a time scale far beyond that typical of molecular motions at or near room temperature. Over time, the superficial population of the probe will diminish as the molecules move fully into the membrane. However, based on relative rates at which the intensities at 435 and 500 nm equilibrate and on the fact that emission at 500 nm never disappears but rather its rate just stabilizes, it is clear that this movement is not the final step of equilibration. Rather, it seems the probe moves to a still shallow location within the bilayer where it remains fairly hydrated. This movement, superficial to shallow, explains why the intensity at 500 nm equilibrates more quickly than at 435 nm for both solid and liquid membranes. Once within the membrane at its shallow location, the probe can then move to a deeper, dehydrated location closer to the center of the bilayer. Patman's emission peak will then be centered at 435 nm, as the fluorophore is no longer in the vicinity of water molecules. This penetration of the probe into a deeper membrane location is likely slow, explaining why hundreds of seconds following the stabilization at 500 nm, the intensity at 435 nm has yet to reach a steady state.

Given the complexity of the equilibration process, it is therefore not surprising that the data required at least three exponential terms in order to be fit. Attempts to fit with only two terms were unsuccessful. However, including a third exponential term was also problematic because the change was so slow that the scalar and rate constant of the third term could not be uniquely defined. Consequently, a linear term was substituted to fit the results. The physical meaning of the third term is unclear. It is possible that it simply represents adsorption of the fluorophore to the walls of the cuvette. This uncertainty is the reason why we used the normalized fit values to calculate the rate

differences. Because of these limitations, we cannot equate the fitting parameters of the experimental results to the model parameters in a meaningful way. This makes the terms of our model phenomenological, rather than explicit.

For Patman, some of the most interesting data was collected at the phase transition temperatures of the saturated lipids. Only under that condition with that probe, did the intensity at 435 nm equilibrate more rapidly than at 500 nm. Additionally, its rapidity of equilibration was dependent on the length of the lipid chain, as Patman equilibrated faster with shorter chains. This may be due to the changes that occur as a lipid molecule passes through its phase transition from a solid-ordered to a liquid-disordered state. The majority of changes occur near the head group of the lipids with the tilt between the heads and chains being altered and the space between the individual lipid heads increasing [21]. In this state of fluctuation, it could be more difficult for a population of probes at the shallow depth to equilibrate than a population at a deeper location, farther from the majority of changes. Additionally, both wavelengths approached equilibrium faster at the phase transition than at either the solid or liquid lipid phases. This could be explained by the destabilization of the state of initial membrane binding. While the lipids transition from an ordered to disordered organization, the initial binding of the probe to the membrane may become less favorable, resulting in a quicker relocation of the fluorophores to positions, whether shallow or deep, within the bilayer.

Laurdan's equilibration at the phase transition differed more from that of Patman's compared to any other lipid state. First, for all three saturated lipid membranes, the difference between the rates remained positive for Laurdan. Second, there was no dependency between lipid chain length and speed of equilibration. Both of these

differences are likely due to the difference in charge between the probes—positive for Patman, neutral for Laurdan. Due to its neutral charge, Laurdan has a tendency to flip from the outer to inner leaflet in single membranes and additionally, through the multiple bilayers in MLVs. Thus, while it may be favorable for Patman, isolated in the outer leaflet, to equilibrate more rapidly at a deeper location (resulting in a negative difference in rates), the data for Laurdan suggest it undergoes not only outer leaflet equilibration but also the flip of the probe to the inner leaflet and additional bilayers. Consequently, despite the destabilization of the shallow location at the phase transition, the intensity at 435 nm requires longer to stabilize than that at 500 nm for Laurdan due to its movement between leaflets.

Saturated vs. Unsaturated Lipids

Another unique characteristic was observed for lipids in the liquid-disordered phase when the data from saturated lipid vesicles and vesicles containing at least 25% unsaturated lipids were compared. Only in this fluid phase for Patman were the rate differences statistically distinguishable for the two types of membranes. The longer equilibration time displayed in the unsaturated membranes may be due to the structure of the lipid tails. The kink resulting from the double bond of unsaturated lipids may somehow hinder the movement of the probe to its deeper, dehydrated location in a liquid membrane and thus, slow the time required from the 435 nm emission curve to stabilize. However, a more in depth investigation is required to fully elucidate this distinction.

Summary

It would appear that when studying the differential equilibration rates of emission intensity at the two edges of the emission spectrum for Patman and Laurdan in living cells that we are studying the ability of the probe to penetrate into the bilayer at various depths. Such an interpretation would provide a valuable understanding to the membrane biophysics involved in the behavior of the dyes. The value of this understanding is emphasized by the original observation that certain changes in the membranes of living cells alter the relative equilibration rates at the two wavelengths. Collecting data immediately upon introduction of a probe to a system, rather than waiting for its equilibration, would enhance and expand our understanding of the biophysical properties of fluorescent probes and their ability to detect changes in the molecular environment.

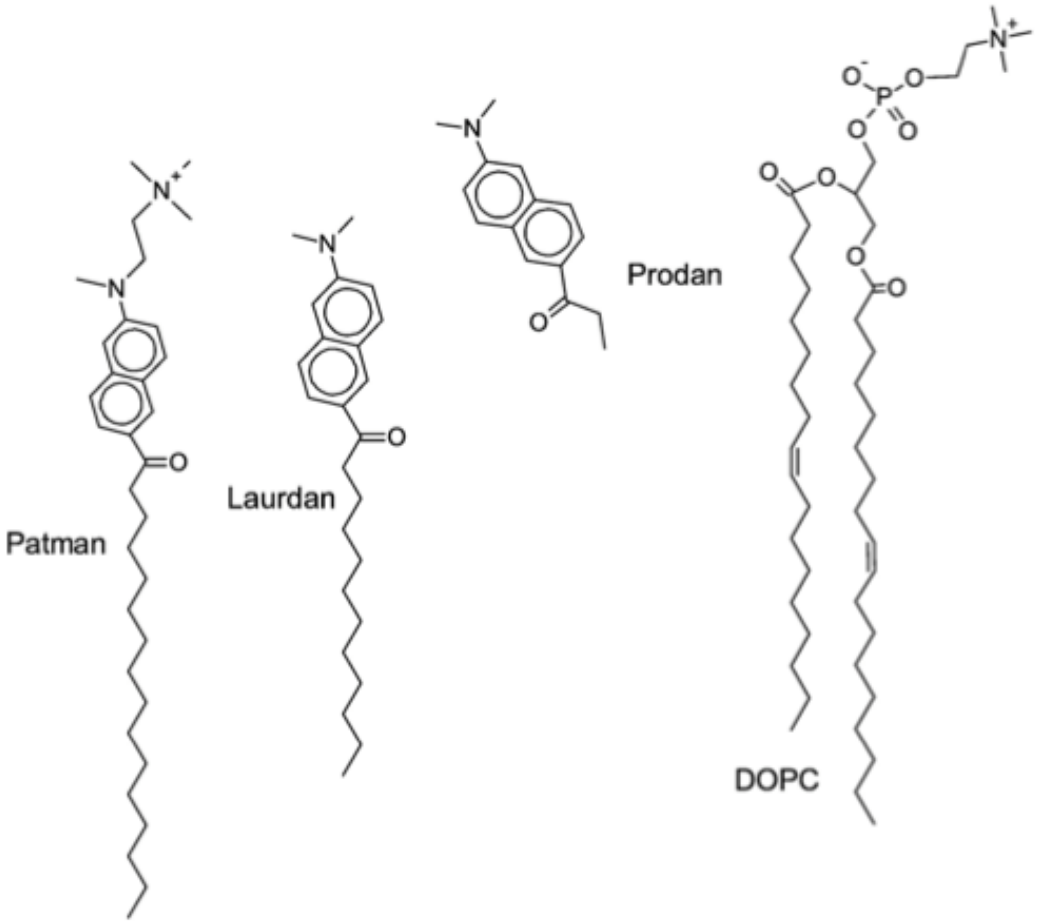

Figure 1: Comparison of the locations of Prodan, Laurdan, and Patman relative to a DOPC lipid molecule (from Rieber et al. 2007) [1]. Patman resides closer to the bilayer center than Laurdan because it has an acyl chain 4 carbons longer and because its benzene rings sit lower along the lipid tail.

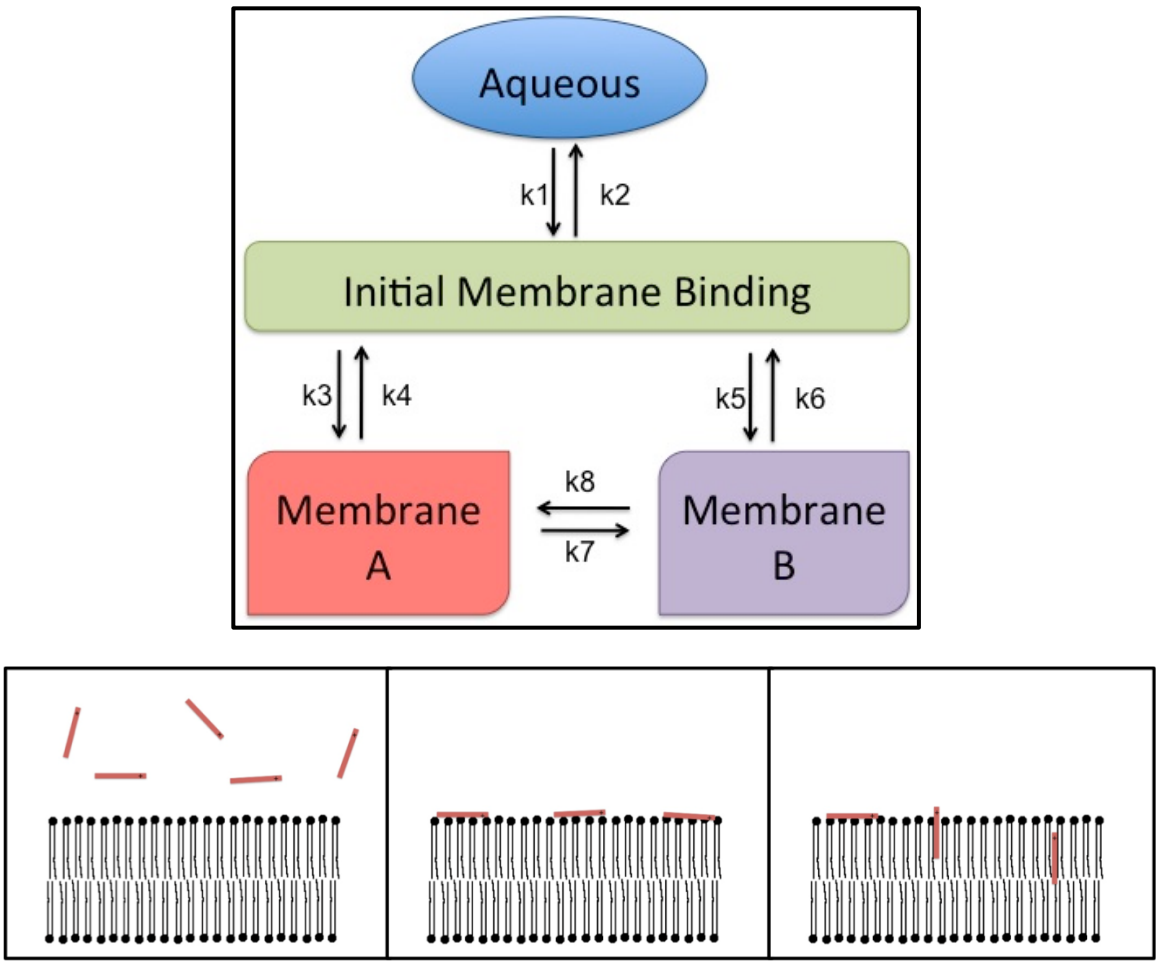

Figure 2: Model displaying the equilibration pathways for Patman and Laurdan in a membrane system (above) and possible mechanism to describe the pathways (below). The proposed depth-dependent explanation of this model is shown in the lower panel (charges added to probe molecules to indicate orientation of the fluorophore with the polar head (positive charge) near the lipid-water interface and the acyl chain oriented toward the bilayer center). The probe is added at time = 0 to the aqueous solution and then quickly moves to bind with available membranes due to unfavorable interactions between the water and the hydrophobic probe. This initial membrane binding is semi-unstable and consequently, is not the final position for the dye. The molecules eventually move fully into the membrane into two discrete positions, Membrane A or Membrane B. As shown in the lower panel, we propose that these two positions represent a shallow, hydrated membrane position for the probe where it undergoes solvent relaxation (500 nm emission peak) and a deeper, more dehydrated position where the probe preferentially emits at a shorter wavelength, 435 nm. Laurdan likely undergoes a more complex equilibration sequence, as it is able to diffuse through the plasma membrane and stain all the membranes in a cell or move through and equilibrate with the multiple leaflets of MLVs. Patman, however, due to its charge, stays in the outer leaflet of the plasma membrane of both cells and MLVs.

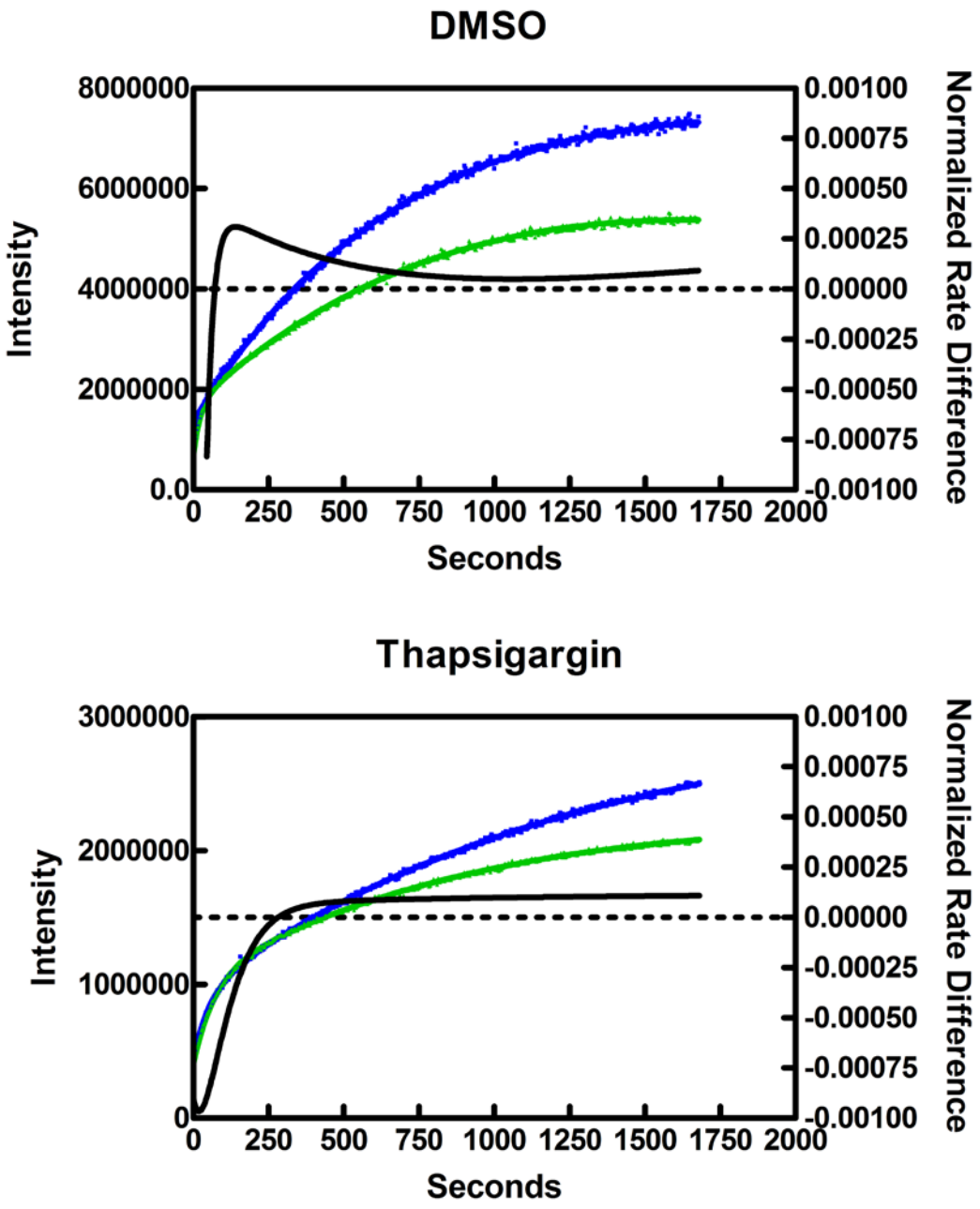

Figure 3: Differential equilibration rates between wavelengths in both healthy and dying cells. The rates of equilibration were monitored for both 435 nm (blue) and 500 nm (green) in healthy cells (upper panel) (treated with dimethyl sulfoxide (DMSO)) or dying, apoptotic cells (lower panel) (treated with thapsigargin). The difference in the normalized rates (Normalized $Rate_{435}$ – Normalized $Rate_{500}$) was calculated (black). Not only did the rates vary between wavelengths, but as the membrane changed with apoptosis, the time course of the rate differences also changed.

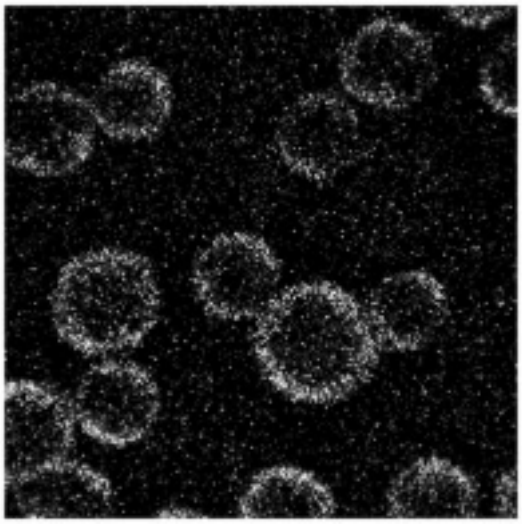

Figure 4: Two-photon data confirms localization of each probe within cellular membranes. Image obtained via two-photon microscopy of S49 lymphoma cells stained with Patman. Pigmentation indicates fluorescence of the dye. The staining pattern of Patman in living cells confirms its localization to the outer leaflet of the plasma membrane due to its positive charge.

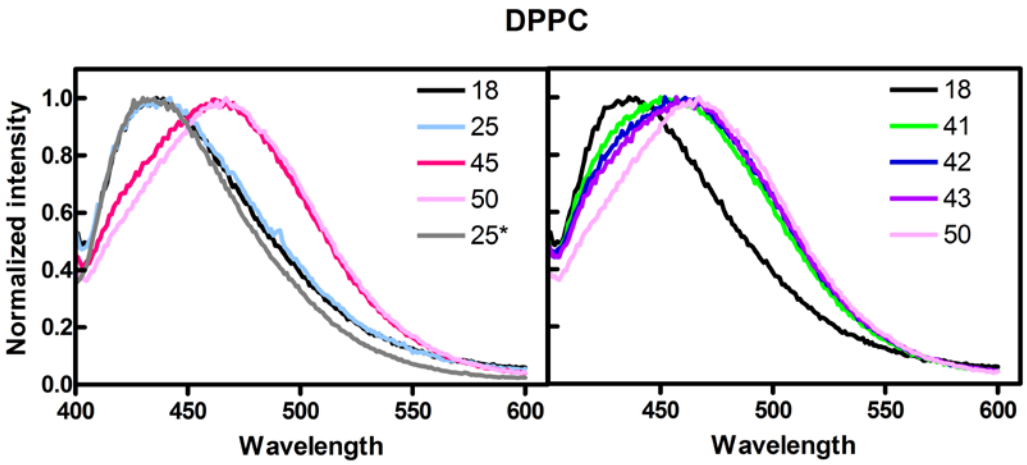

Figure 5: Normalized Patman emission spectra in DPPC. Patman was added to the MLV system of DPPC at 18 °C and allowed to equilibrate through a 1000 s time course. Left Panel: Spectra were collected at low, 18 (black) and 25 °C (blue), and high temperatures, 45 (pink) and 50 °C (pale pink). Following acquisition of the highest temperature (50 °C), the system was cooled back down to 25 °C (grey, denoted as 25*), and an emission spectrum was gathered. Right Panel: Spectra were also acquired at temperatures just around the phase transition, 41−43 °C, (green, dark blue, purple; reference lines included at 18 and 50 °C).

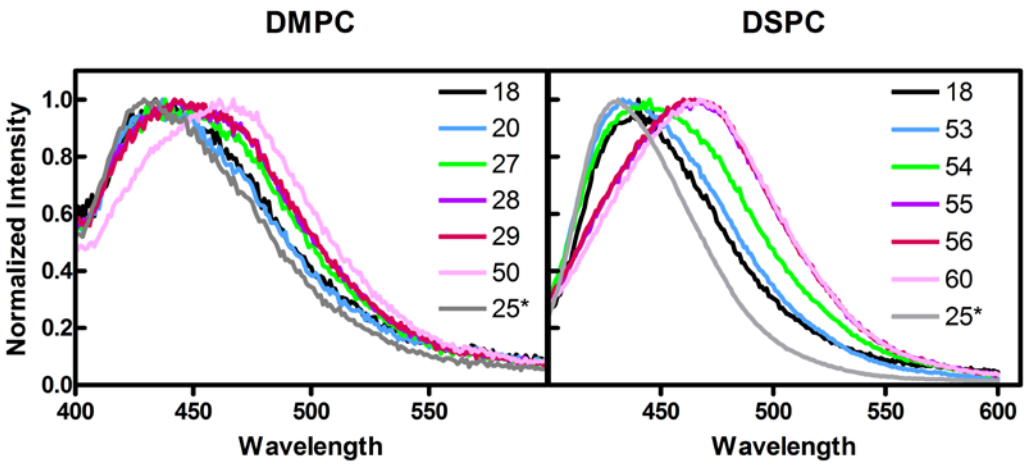

Figure 6: Normalized Patman emission spectra in DMPC and DSPC. Patman was added to the MLV system of DMPC or DSPC at 18 °C and allowed to equilibrate through a 1000 s time course. Left Panel: For DMPC, spectra were collected at low, 18 and 20 °C (black and blue), and high temperatures, 50 °C (pale pink), as well as temperatures surrounding the phase transition, 27−29 °C, (green, purple, pink). Right Panel: For DSPC, spectra were collected at low, 18 °C (black), and high temperatures, 60 °C (pale pink), along with those including and around the phase transition temperature, 53−56 °C (blue, green, purple, pink). For both types of vesicles, following acquisition of the highest temperature spectrum, the systems were cooled back to 25 °C (grey, denoted as 25*), and spectra were gathered.

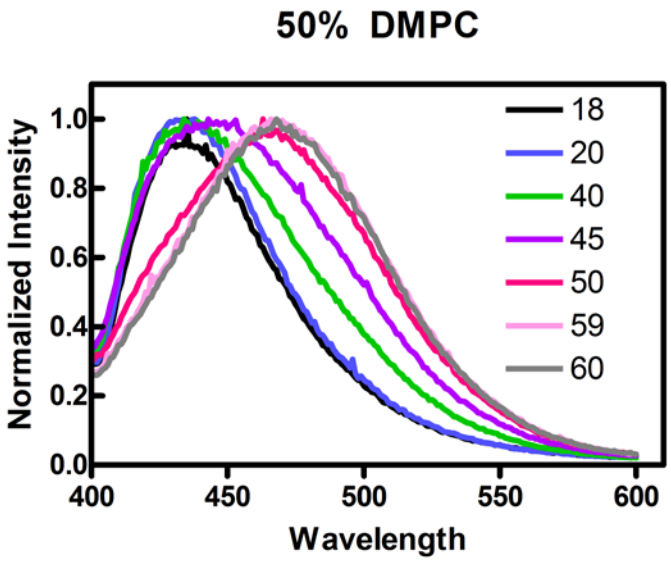

Figure 7: Normalized Patman emission spectra of vesicles composed of 50% DMPC-50% DSPC. Patman was added to a mixed MLV system containing equal parts DMPC and DSPC and allowed to equilibrate through a 1000 s time course. Spectra were collected at low, 18 and 20 °C (black and blue), and high temperatures, 59 and 60 °C (pale pink and grey), as well as temperatures between the two individual phase transitions, 40−50 °C (green, purple, pink).

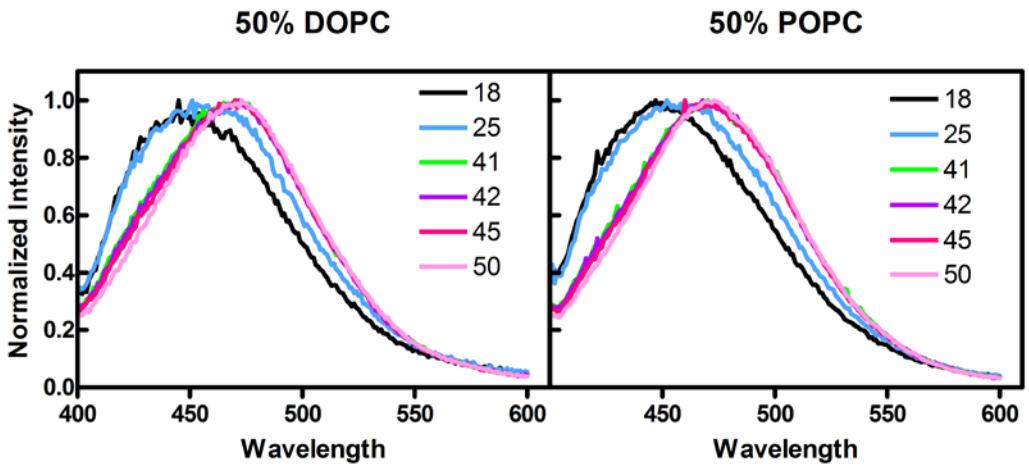

Figure 8: Normalized Patman emission spectra of vesicles with unsaturated lipids and DPPC. Patman was added to a mixed MLV system containing equal parts DPPC and unsaturated lipids (either DOPC or POPC) and allowed to equilibrate through a 1000 s time course. Left Panel: For 50% DOPC vesicles, spectra were collected at low, 18 and 25 °C (black and blue), and high temperatures, 45 and 50 °C (pink and pale pink). Spectra were also collected surrounding the phase transition temperature of DPPC, 41 and 42 °C (green and purple). Right Panel: For 50% POPC vesicles, spectra were collected at low, 18 and 25 °C (black and blue), and high temperatures, 45 and 50 °C (pink and pale pink). Spectra were also collected surrounding the phase transition temperature of DPPC, 41 and 42 °C (green and purple).

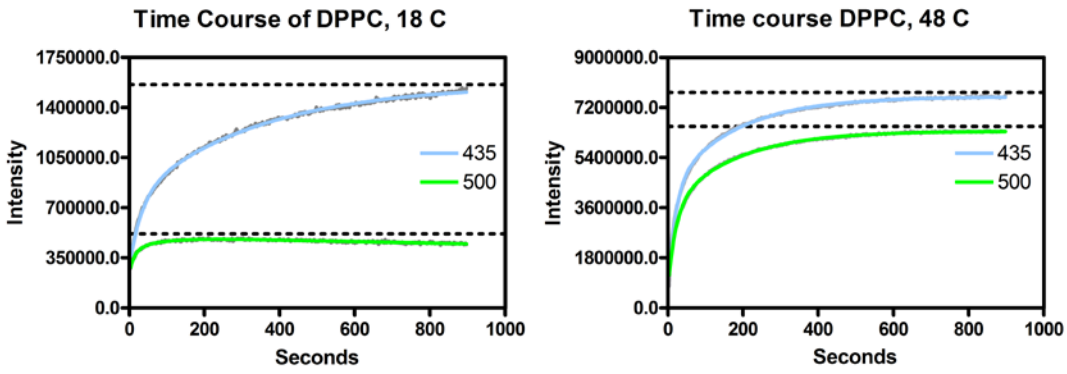

Figure 9: Emission time courses of Patman in DPPC vesicles at temperatures in the solid-ordered and liquid-disordered membrane phases. Patman was added at time zero, and the emission intensities of 435 and 500 nm were assayed at 18 (Right Panel) and 48 °C (Left Panel) in MLV DPPC membranes. Reference lines (dotted lines) were added just above the end point fluorescence to aid with visualization of stabilization. Data were fit with a non-linear regression equation (see *Materials and Methods*) for each wavelength (435 nm (blue) and 500 nm (green)).

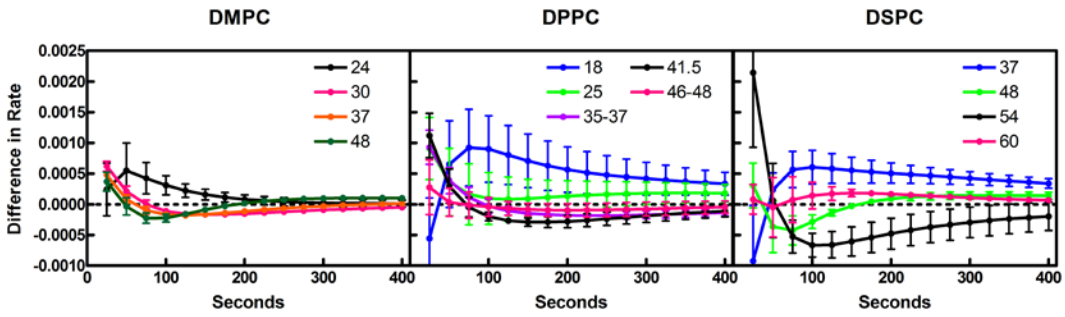

Figure 10: Time courses of difference in rates for Patman equilibration in saturated, single-component membranes. The derivatives of the normalized fits from the emission time courses were calculated (see *Materials & Methods*) from 0 to 400 s. Data shown represent the solid-ordered phase of the individual membranes (DPPC: 18, 25, 35−37 °C (blue, green, purple); DSPC: 37 and 48 °C (blue and green)), the phase transition temperatures of each system (DPPC: 41.5 °C; DMPC: 24 °C; DSPC: 54 °C (black)), and the liquid-disordered phases (DMPC: 30, 37, and 48 °C (pink, orange, dark green); DPPC: 46–48 °C (pink); DSPC: 60 °C (pink)). Error bars represent SEM (n = 6).

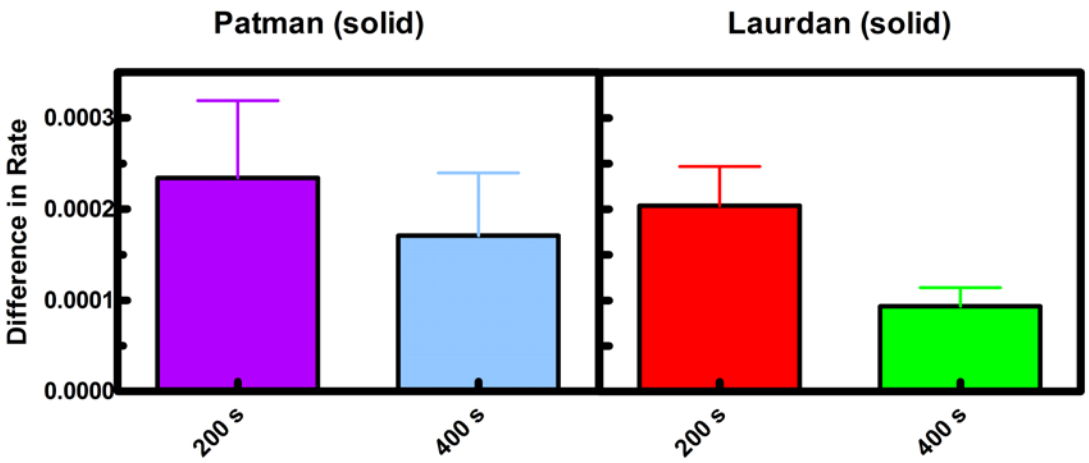

Figure 11: Differences in normalized equilibration rates of solid-ordered membranes for both Patman and Laurdan. Rate differences were calculated as previously explained for a variety of vesicles composed of phosphatidylcholine species, including myristic, palmitic, or steric side chains, comprising either one- or two-component membranes. Data from time courses at temperatures below the published main phase transition were pooled (n = 31–81). The results represent the rate difference at 200 or 400 s after the addition of either Patman (Left Panel) or Laurdan (Right Panel).

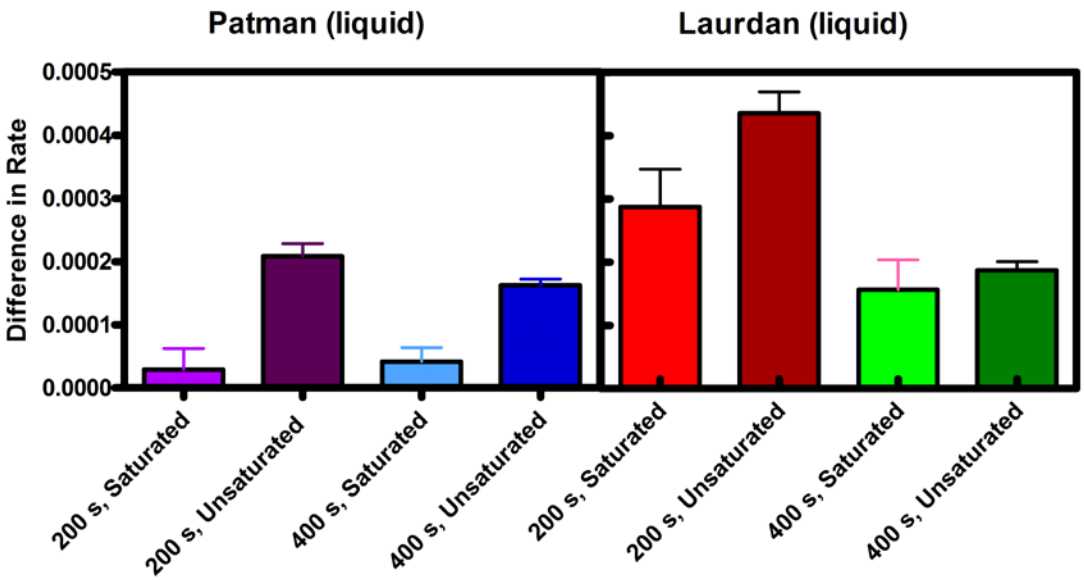

Figure 12: Differences in normalized equilibration rates of liquid-disordered membranes for both Patman and Laurdan. Rate differences were calculated as previously explained for a variety of vesicles composed of phosphatidylcholine species, including myristic, palmitic, or steric side chains, comprising either one- or two-component membranes. For Patman, data from time courses at temperatures above the published main phase transition were pooled for entirely saturated membranes (purple and blue) or membranes containing at least 25% unsaturated lipids (dark purple and dark blue) (n = 36–58). For Laurdan, data for entirely saturated membranes (red and green) or membranes containing at least 25% unsaturated lipids (dark red and dark green) (n = 28–33). The results represent the rate difference at 200 or 400 s after the addition of either Patman (Left Panel) or Laurdan (Right Panel).

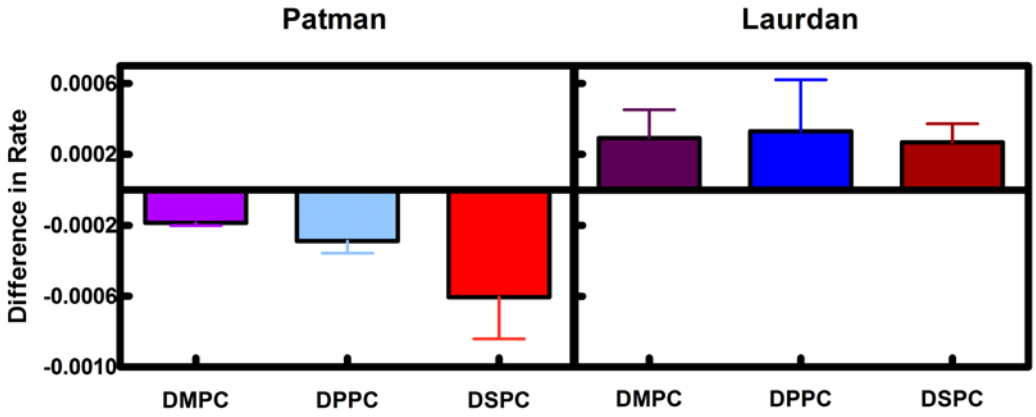

Figure 13: Differences in normalized equilibration rates of membranes of saturated lipids at their phase transition temperatures for both Patman and Laurdan. Rate differences were calculated as previously explained for single-component, saturated phosphatidylcholine membranes (DMPC – 14:0, DPPC – 16:0, DSPC – 18:0). Data from experiments carried out at each respective published phase transition were pooled (n = 3–6). The results represent the rate difference at 150 s after the addition of either Patman (Left Panel) or Laurdan (Right Panel).

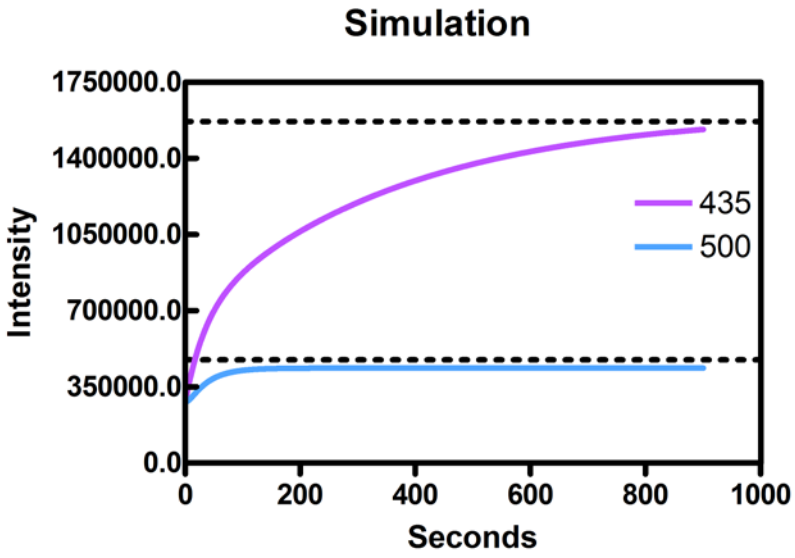

Figure 14: Numerical simulation of the model shown in Figure 2 with parameters set to model the data in Figure 9 (Left Panel). Parameters set to quickly move the probe out of aqueous solution where it barely fluoresces to a membrane environment, where its fluorescence is much greater. (Rate constants: k1 = 0.015, k2 = 1.5e-6, k3= 0.0025, k4 = 0.00025, k5 = 0.1, k6 = 0.01, k7 = 0.00001, k8 = 0.00001) (Relative fluorescence Values: Aqueous: 435 nm = 280, 500 nm = 280; Initial Membrane Binding: 435 nm = 1200, 500 nm = 300; Membrane A: 435 nm = 3100, 500 nm = 300; Membrane B: 435 nm = 300, 500 nm = 600)

WORKS CITED

1. Rieber, K., et al., *The use of solvent relaxation technique to investigate headgroup hydration and protein binding of simple and mixed phosphatidylcholine/surfactant bilayer membranes.* Biochimica et Biophysica Acta (BBA) - Biomembranes, 2007. **1768**(5): p. 1050-1058.
2. Piotr Jurkiewicz, A.O., Marek Langner, and Martin Hof, *Headgroup Hydration and Mobility with DOTAP/DOPC: A Fluorescence Solvent Relaxation Study.* Langmuir, 2006. **22**: p. 8741-8749.
3. Olzynska, A., et al., *Molecular interpretation of fluorescence solvent relaxation of Patman and 2H NMR experiments in phosphatidylcholine bilayers.* Chemistry and Physics of Lipids, 2007. **147**(2): p. 69-77.
4. Hof, R.H.a.M., *Dynamics in Diether Lipid Bilayers and Interdigitated Bilayer Structures Studied by Time-Resolved Emission Spectra, Decay Times, and Anisotropy Profiles* Journal of Fluorescence, 2001. **11**(3).
5. Rudi Hutterer, A.B.J.P., and Martin Hof, *Solvent Relaxation of Prodan and Patman: A Useful Tool for the Determination of Polarity and Rigidity Changes in Membranes.* Journal of Fluorescence, 1998. **8**(4).
6. Sykora, J., et al., *Influence of the curvature on the water structure in the headgroup region of phospholipid bilayer studied by the solvent relaxation technique.* Chemistry and Physics of Lipids, 2005. **135**(2): p. 213-221.
7. Jana Humpolickova, M.S., Karel Prochazka, and Martin Hof, *Solvent Relaxation Study of pH-Dependent Hydration of Poly(oxyethylene) Shells in Polystyrene-block-poly(2-vinylpyridine)-block-poly(oxythylene) Micelles in Aqueous Solutions.* Journal of Physical Chemistry A, 2005. **109**: p. 10803-10812.
8. R. Hutterer, F.W.S., H. Sprinz, M. Hof, *Binding and relaxation behaviour of prodan and patman in phospholipid vesicles: fluorescence and H NMR study* Biophysical Chemistry, 1996. **61**: p. 151-160.
9. Bagatolli, L., *To see or not to see: Lateral organization of biological membranes and fluorescence microscopy.* Biochimica et Biophysica Acta (BBA) - Biomembranes, 2006. **1758**(10): p. 1541-1556.
10. Lúcio, A.D., et al., *Laurdan Spectrum Decomposition as a Tool for the Analysis of Surface Bilayer Structure and Polarity: a Study with DMPG, Peptides and Cholesterol.* Journal of Fluorescence, 2009. **20**(2): p. 473-482.
11. Moyano, F., J.J. Silber, and N.M. Correa, *On the investigation of the bilayer functionalities of 1,2-di-oleoyl-sn-glycero-3-phosphatidylcholine (DOPC) large unilamellar vesicles using cationic hemicyanines as optical probes: A wavelength-selective fluorescence approach.* Journal of Colloid and Interface Science, 2008. **317**(1): p. 332-345.
12. Joseph R. Lakowicz, D.R.B., Badri P. Maliwal, Henryk Cherek, and Aleksander Baiter, *Synthesis and Characterization of a Fluorescence Probe of the Phase Transition and Dynamic Properties of Membranes.* Biochemistry, 1983. **22**: p. 9.
13. Farris, G.W.a.F.J., *Synthesis and spectral properties of a hydrophobic fluorescent probe- 6-propionyl-2-(dimethylamino)naphthalene.* Biochemistry, 1979. **18**: p. 4.
14. SS Antollini, F.B., *Laurdan studies of membrane lipid-nicotinic acetylcholine receptor protein interactions.* Methods in Molecular Biology, 2007. **400**: p. 12.

15. Kapoor S, W.A., Denter C, Zhai Y, Markgraf J, Weise K, Opitz N, Winter R, *Temperature-pressure phase diagram of a heterogeneous anionic model biomembrane system: Results from a combined calorimetry, spectroscopy and microscopy study.* Biochim Biophys Acta, 2011. **1808**(4): p. 9.
16. Granjon T, V.M., Vial C, Buchet R, *Mitochondrial creatine kinase binding to phospholipids decreases fluidity of membranes and promotes new lipid-induced beta structures as monitored by red edge excitation shift, laurdan fluorescence, and FTIR.* Biochemistry, 2001. **40**(20): p. 11.
17. Hannabeth A. Franchino, B.C.J., Steven K. Neeley, Rajeev B. Tajhay, Mai P. Vu, Heather A. Wilson-Ashworth, and John D. Bell, *Combined use of steady state fluorescence emission and anisotropy of merocyanine 540 to distinguish crystalline, gel, ripple, and liquid crystalline phase in dipalmitoylphosphatylcholine bilayers* PMC Biophysics, 2010. **3**(14): p. 16.
18. Erin D. Olson, J.N., Katalyn Griffith, Thaothanh Nguyen, Michael Streeter, Heather A. Wilson-Ashworth, Michael H. Gelb, Allan M. Judd, and John D. Bell, *Kinetic evaluation of cell membrane hydrolysis during apoptosis by human isoforms of secretory phospholipase A2.* J Biol Chem, 2010. **285**(5): p. 10.
19. Heather A. Wilson, W.H., Jacqueline B. Waldrip, Allan M. Judd, Leo P. Vernon, John D. Bell, *Mechanisms by which thionin induces susceptibility of S49 cell membranes to extracellular phospholipase A 2.* Biochimica et Biophysica Acta (BBA) - Biomembranes, 1997. **1349**(2): p. 15.
20. Bailey, R.W., et al., *Sequence of Physical Changes to the Cell Membrane During Glucocorticoid-Induced Apoptosis in S49 Lymphoma Cells.* Biophysical Journal, 2009. **96**(7): p. 2709-2718.
21. Yeagle, P., *The Structure of Biological Membranes*1992, Boca Raton, FL: CRC Press.

Curriculum Vitae

Hannabeth Franchino
411 West 28th Avenue
Spokane, WA 99203
(509)590-8502
hbfranchino@gmail.com

Education

Master of Science, Physiology and Developmental Biology
Brigham Young University, Provo, UT
Graduation: June 2011

Bachelor of Science, Biology (graduated with Honors & Cum Laude)
Brigham Young University, Provo, UT
Graduation: April 2010

Research Experience

• April 2010 − April 2011 • BYU Physiology and Developmental Biology Department • Provo, UT •

Thesis Project: Possible Molecular Mechanism to Account for Wavelength Dependence of Equilibration Rates of Patman and Laurdan in Phosphatidylcholine Bilayers.

- Fluorescence spectroscopy experiments with plasma membrane probes in artificial membranes; data analysis; creation of computer simulation model to replicate experimental results; publication and defense of thesis; preparation of publication for a peer-reviewed journal

• September 2007 − April 2010 • BYU Physiology and Developmental Biology Department • Provo, UT •

- Fluorescence spectroscopy experiments with a plasma membrane probe in artificial membranes; data analysis; writing, preparing, and publishing a publication in a peer-reviewed journal

Publications

Franchino HA, Johnson BC, Neeley SK, Tajhya RB, Vu MP, Wilson-Ashworth HA, Bell JD. *"Combined use of steady-state fluorescence emission and anisotropy of merocyanine 540 to distinguish crystalline, gel, ripple, and liquid crystalline phases in dipalmitoylphosphatidylcholine bilayers."* PMC Biophysics, 2010. 3(14): p 16.

Presentations

"A complete phase diagram for palmitoylphingomyelin-cholesterol liposomes." 52nd Biophysical Society Annual Meeting, 2008; Long Beach, CA

"Assessment of Merocyanine Subpopulations in DPPC Vesicles Using Anisotropy and Lifetime Measurements." 53rd Biophysical Society Annual Meeting, 2009; Boston, MA

"Combined use of steady-state fluorescence emission and anisotropy of merocyanine 540 to distinguish crystalline, gel, ripple, and liquid crystalline phases in dipalmitoylphosphatidylcholine bilayers." 54th Biophysical Society Annual Meeting, 2010; San Francisco, CA

"Relationships between Bilayer Phase and Equilibration Rates of Patman and Laurdan." 55th Biophysical Society Annual Meeting, 2011; Baltimore, MD

Scholarships & Funding

• Research Assistantship • BYU PDBio Dept. • Winter Semester 2011

• Research Assistantship • Dr. John Bell, NIH Grant GM073997 •
• April 2010 − December 2010 •

• Recipient of Heritage (Full Tuition) Scholarship from BYU •
• September 2006 − April 2010 •

• Recipient of Spokane Scholar Science Award and $1500 Scholarship •
• March 2006 •